CHEMISTRY

Spraying of water microdroplets forms luminescence and causes chemical reactions in surrounding gas

Yifan Meng[1], Yu Xia[1,2]*, Jinheng Xu[1], Richard N. Zare[1]*

When neutral water is sprayed, oppositely charged microdroplets are formed. The close approach of oppositely charged microdroplets causes an electrical discharge and leads to luminescent emission. The light emission happens without any external voltage applied, and the electrical discharge is sufficiently energetic to excite, dissociate, or ionize surrounding neutral gas molecules. Thus, sprayed water microdroplets cause chemical reactions to occur. Similar findings to the Urey-Miller experiment were observed by spraying room temperature water microdroplets into a gas mixture containing nitrogen, methane, carbon dioxide, and ammonia, which leads to the synthesis of organic molecules containing carbon-nitrogen (C—N) bonds. These observations provide another explanation for unique reactivity at the gas-water interface, as well as a possible mechanism for making the building blocks of life on early Earth.

INTRODUCTION

Pure water is known to be a poor conductor of electricity caused by the lack of charge carriers compared to the number of neutral molecules. However, in 1867, Lord Kelvin (William Thomson) built an electrostatic device to generate sparks between two metal buckets that collected falling streams of water droplets originating from the same water reservoir suspended over the buckets (*1*). This paradoxical behavior is caused by charge separation (*2*). In storm clouds, electrical separation resulting from turbulent motion of small soft ice pellets and collision between water droplets and ice crystals also leads to electrical separation that builds up until electrical breakdown of air occurs, which manifests itself as lightning (*3*). We also note that there is published evidence supporting the coexistence of positive and negative droplets in aqueous aerosols (*4*).

It is common in nature that water droplets are charged. This is attributed to contact electrification (*5*–*8*) that occurs when two different phases touch, specifically when water contacts some hydrophobic medium, such as air, oil, or insoluble mineral. As first observed by Lenard in 1892 by examining the charge on water droplets at the base of a waterfall (*9*), it has been confirmed in many studies that, when water is sprayed, smaller droplets are negatively charged whereas larger droplets are positively charged (*10*, *11*). On a single droplet, shear forces generate small negative droplets from the water surface, leaving a positive charge on the remaining larger fragment. A video of this process has been made available, which allows the easy visualization (*12*).

Recently, Banerjee and co-workers found that sprayed water microdroplets could cause the ionization of gas molecules in air (*13*). In this study, we present evidence that, when oppositely charged water droplets come close together, electrons jump between them, causing an electrical discharge accompanied by photon emission. It might be wondered what the mechanism is that causes this luminescence. It has been suggested that one possibility is Cherenkov radiation, which occurs when the motion of charged particles exceeds the speed of light in the medium (*14*, *15*). The speed of light in air is almost the same as that in a vacuum, and the speed of light in water is about 75% of that in vacuum. Experiments in which a water microdroplet spray is surrounded by argon demonstrate that any Cherenkov radiation present was below our detection limit (movie S1). Instead, we believe that luminescence arises by emission from excited electronic states caused by electron impact excitation. Thus, this process exhibits the same properties as lightning in air, for example, the ability to excite, dissociate, and ionize molecules. Therefore, we have named this phenomenon as "microlightning." This observation offers an interesting explanation for the unique reactivity at the water-gas interface (*16*–*19*). Furthermore, this microlightning from spayed water droplets can lead to similar results concerning the prebiotic synthesis of small organic molecules as first reported by Miller and Urey in their classic bulb-discharge experiments (*20*, *21*). Specifically, when spaying water droplets into a gas mixture of N_2, CH_4, CO_2, and NH_3, we have found the formation of organic molecules containing C—N bonding, such as hydrogen cyanide (HCN), the amino acid glycine (NH_2CH_2COOH), and the cyclic molecule uracil ($C_4H_4N_2O_2$), which is one of the four nucleotide bases in RNA (*22*). These reactions can occur in less than 200 μs. Given that lightning is an intermittent and unpredictable phenomenon, whereas water sprays are so common on Earth, we suggest that our results provide another possible pathway for the abiotic formation of C—N bonds.

RESULTS

Luminescent emission

It is well known that an electrical discharge in air produces light energy (*23*). In this study, we found that the splitting of water into larger and smaller droplets, which carry opposite charges, leads to an electrical discharge that emits photons. To detect photon emission from the splitting of a single microdroplet, we built an acoustic setup, which can levitate a single water microdroplet and induce droplet splitting (Fig. 1A). Two copper electrodes were mounted on opposite sides. By using a syringe, a single water droplet with a certain volume can be added to the acoustic levitation area, which is between the transmitter and the reflector. A high-speed camera (FASTCAM NOVA R3-4K, Photron, Shanghai, China) was used to capture the motion of the droplets at 20,000 fps. Sound waves levitate the droplet in the air (Fig. 1B). A supplementary video shows

[1]Department of Chemistry, Stanford University, Stanford, CA 94305, USA. [2]School of Environment and Health, Jianghan University, Wuhan 430056, China.
*Corresponding author. Email: zare@stanford.edu (R.N.Z.); xiayu@jhun.edu.cn (Y.X.)

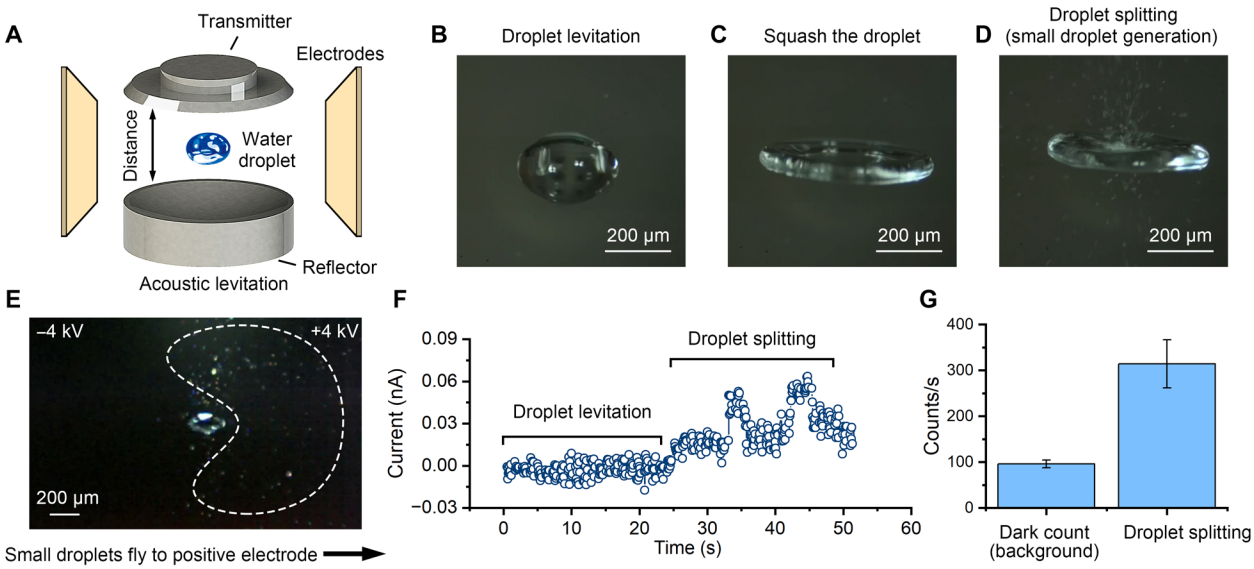

Fig. 1. Detection of luminescence from water microdroplet fission. (**A**) Experimental setup of droplet levitation. Photos of (**B**) droplet levitation, (**C**) squashed droplet, and (**D**) droplet splitting by controlling the distance between the transmitter and reflector in (A). (**E**) Photo of droplet splitting when applying a voltage on the two electrodes shown in (A). The generated small droplets fly to the positive electrode (outlined in white). (**F**) Light detection by a photon amplified detector from droplet splitting. (**G**) Light detection by a photon counter from droplet splitting.

that the droplet is constantly rotating under the control of the sound field (movie S2). Now, multiple mechanisms have been proposed to explain why droplets become charged, such as gas-liquid contact (*24*), solid-liquid contact (*25*), and three-phase contact (*26*). Here, we propose that the contact electrification between the droplet and the surrounding air is one of the primary reasons for the droplet's initial charge as the droplet's interface is only in contact with air during levitation. During the contact process between the droplet and the air, the original large droplet becomes positively charged from the loss of electrons (fig. S1 and movie S3). It is worth noting that the evaporation of neutral water molecules can lead to an increase in droplet charge density. However, during the 15-s measurement period, almost no reduction in droplet volume was observed. Therefore, the effect of water evaporation was not considered. By reducing the distance between the transmitter and the reflector, the droplet can be squashed (Fig. 1C). With further reduction of the distance, the original large water droplet split into several smaller droplets (Fig. 1D and movie S4). In the demonstration shown in Fig. 1 (B to D), both electrodes are grounded. As a result, the generated water microdroplets shown in Fig. 1D flew outward in all directions. Figure 1E shows a different phenomenon when a potential of −4 kV is applied to the left electrode and +4 kV to the right electrode. As shown in the white outlined area, all the generated water microdroplets fly toward the positive electrode driven by electrostatic attraction, confirming that the small droplets are negatively charged (movie S5). When larger positively charged droplets and smaller negatively charged droplets approach sufficiently close to one another (i.e., at the beginning of the splitting process), it is expected that electrons will jump between the oppositely charged droplets, and the surrounding gases will break down, behaving like a plasma.

A photon amplified detector (PDA36UV, DOSpectrum, Chengdu, China) was used to detect the photon emission from oppositely charged water microdroplets approaching to each other. The whole setup was placed in a dark room, and both electrodes were grounded. As shown in Fig. 1F, from 0 to 25 s, the distance between the transmitter and the reflector is controlled appropriately to keep the droplet levitating. During this period, we did not observe any luminescent emission. From 25 to 50 s, we reduced the distance between the transmitter and the reflector to generate smaller droplets from the larger one. A marked luminescence can be observed. To confirm further this finding, we carried out experiments using a photon counter (H8259, Hamamatsu Photonics, Japan) under the same conditions. As shown in Fig. 1G, when the droplet is levitated, the number of photons detected by the photomultiplier tube is about 100 counts/s (dark count). When the droplet splits, the number of photons increased to 300 counts/s. In a dark environment, the high-speed camera also captured the light emitted by the water microdroplets (movie S6). Further proof is provided by viewing the falling of a water microdroplet as it splashes on contact with polytetrafluoroethylene surface, as shown in movies S7 and S8. These results directly demonstrate that an electrical discharge occurs during the splitting of a single water droplet, leading to the generation of photons.

Ionization of neutral species by water droplet microlightning

Another common application of discharges is to generate plasma, thereby ionizing gas molecules or atoms (*27*, *28*). Unlike a conventional protonation or deprotonation ionization process, the discharge can cause gas molecules or atoms to lose their outermost electrons, resulting in the formation of the corresponding positive ions. We used this characteristic to evaluate the ionization ability of the microlightning occurring between oppositely charged water microdroplets. The experimental setup and more details are shown in note S1 and fig. S2. Here, we used a water spray rather than a single water droplet. The charge separation phenomenon can also be observed by using this droplet generation method (fig. S3). Figure 2A shows results of the simulation for the electric field in the gap of a larger positively charged droplet (16 μm in diameter) and a smaller negatively charged droplet (4 μm in diameter) obtained from Comsol 6.1 (Burlington, MA, US)

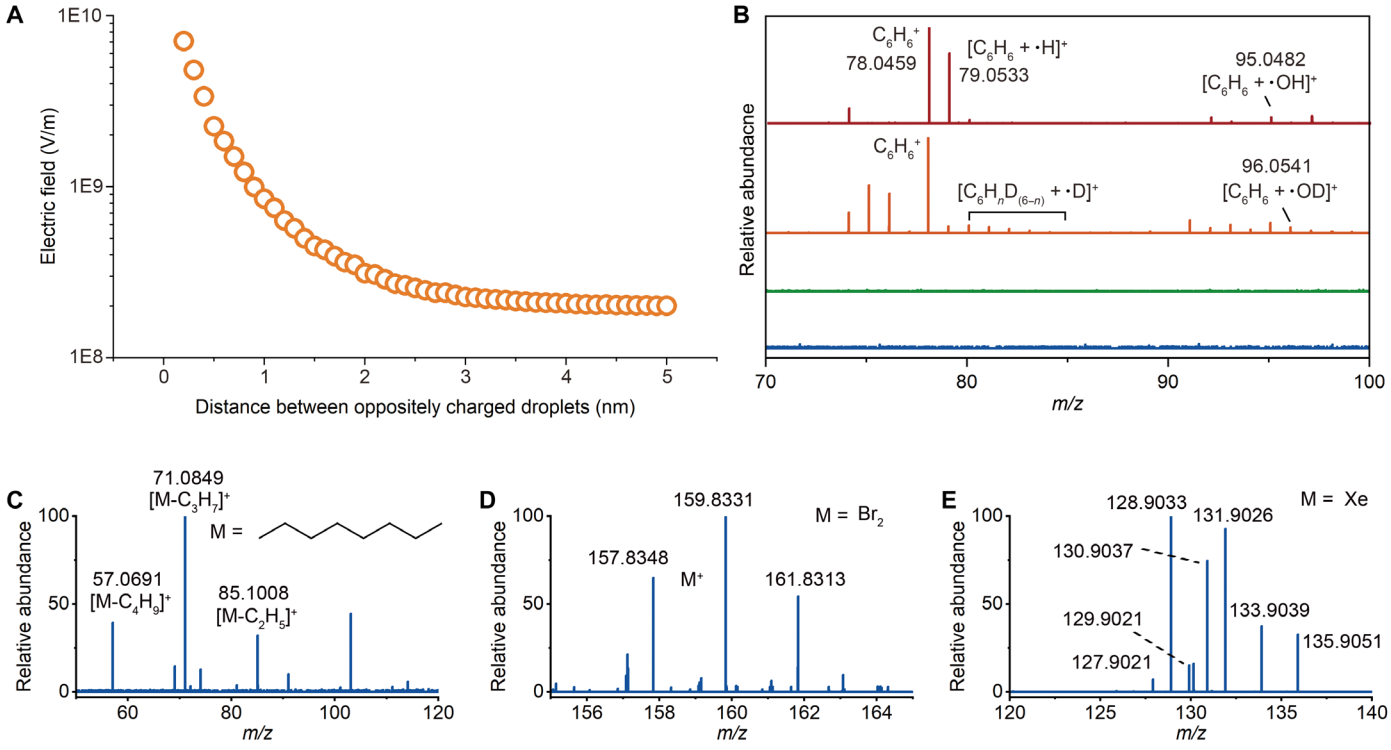

Fig. 2. Ionization ability water droplet microlightning. (**A**) Simulation of electric field between two oppositely charged microdroplets. (**B**) Ionization of benzene vapor by microlightning. Mass spectrum of the chemical components in the chamber while evaporating benzene (blue), evaporating benzene and injecting N_2 (green), evaporating benzene and injecting H_2O microdroplets nebulized by N_2 (orange), evaporating benzene, and injecting D_2O nebulized by N_2 (red). Mass spectrum in positive mode obtained from (**C**) octane (C_8H_{18}), (**D**) bromine (Br_2), and (**E**) xenon (Xe) ionized by the water droplet microlightning.

when changing the distance from 0.1 to 5 nm. From this result, the electric field between two oppositely charged water microdroplets is calculated to exceed 8×10^9 V/m. We expect that fluctuations in the size of droplets will generate an electric field even stronger. Details of the simulation and the estimation of the total charge of the droplets are consistent with a previous study (*12*).

Figure 2B shows the chemical component in the chamber by using mass spectrometry (MS). Because air has been removed from the chamber, there are only water microdroplets, nitrogen molecules, and benzene molecules (C_6H_6) in the gas phase. We carried out a series of experiments to prove that benzene can only be ionized in the presence of water microdroplets. The blue line in Fig. 2B represents the mass spectrum of benzene vapor without injecting water or N_2 from the droplet generator, in which we did not observe any ions. The green line in Fig. 2B represents the mass spectrum of benzene vapor and N_2 without water injection. It shows that the collision between N_2 and gaseous benzene molecules cannot generate benzene positive ions. Benzene entered the mass spectrometer in the form of neutral molecules. However, when we injected water from the fused silica capillary at a flow rate of 10 μl/min and generated microdroplets inside the chamber, benzene positive ions were detected by the mass spectrometer. As shown in the red line in Fig. 2B, a peak at mass/charge ratio (*m/z*) 78.0459 is detected, which is identified to be $C_6H_6^+$, the ion formed from the loss of an electron from the benzene molecule. In addition, we also observed peaks at *m/z* 79.0533 and 95.0428, which are $C_6H_7^+$ and $C_6H_7O^+$, respectively. Here, $C_6H_7^+$ at *m/z* 79.0533 is thought to be the adduct of the benzene cation ($C_6H_6^+$) and a hydrogen radical, whereas $C_6H_7O^+$ at *m/z* 95.0428 is the adduct of $C_6H_6^+$ and a hydroxyl radical. This observation further provides experimental support for the formation of •H and •OH at the water microdroplet–gas interface (*29*).

We also explored the effects of replacing H_2O with D_2O. As shown by the orange line in Fig. 2B, the $C_6H_6^+$ signal at *m/z* 78.0459 still exists because of the microlightning between two oppositely charged D_2O microdroplets. Similarly, ions of $[C_6H_6 + \cdot D]^+$ and $[C_6H_6 + \cdot OD]^+$ at *m/z* of 80.0602 and 96.0541 can be detected, in which the benzene cation ($C_6H_6^+$) acts as the radical scavenger of •D and •OD. In addition, hydrogen-deuterium exchange on the benzene ring can be detected in this system, shown in Fig. 2B.

It is well known that the first ionization potential (IP) of a molecule is the energy needed to remove the outermost, lowest energy electron from the neutral molecule in the gas phase. As shown in Eq. 1, the first IP of benzene is 9.24 eV

$$C_6H_6(g) \rightarrow C_6H_6^+(g) + e^- \qquad IP = 9.24\ eV \qquad (1)$$

We have directly observed $C_6H_6^+$ by in situ MS. This result represents a lower bound to the energy of microlightning, i.e., the potential difference between oppositely charged droplets, which is found to exceed the first ionization energy of benzene. Figures S4 to S6 provide more examples of the ionization of gaseous molecules containing a benzene ring by water droplet microlightning.

We also investigated the ionization of other nonpolar molecules or atoms by the water droplet microlightning. Figure 2C shows the mass spectrum of chemical components in the chamber while we

spray water microdroplets and evaporate octane, whose first IP is 10.25 eV (*30*). As shown in the spectrum, the fragment peaks of octane are detected, which are $[M\text{-}C_2H_5]^+$ at *m/z* 85.1005, $[M\text{-}C_3H_7]^+$ at *m/z* 71.0849, and $[M\text{-}C_4H_9{}^+]$ at *m/z* 57.0691. The reason for the absence of M^+ here is the poor stability of the straight-chain alkane cation, which matches the EI (electron impact)–MS spectrum of octane (*31*). Figure 2D displays the mass spectrum when we introduce bromine (Br_2; first IP = 10.55 eV). Br_2 is known to react with water microdroplets to form HBr and HBrO, but when we detect ions in positive mode, we found $Br_2{}^+$. The microlightning between oppositely charged microdroplets is also strong enough to ionize xenon (Xe), which is a rare gas and has a high first IP at 12.13 eV (Fig. 2E). Xe is directly introduced into the chamber with a flow meter from a cylinder. It is worth mentioning that we cannot observe a signal of Kr^+ when we introduce Kr to the chamber, which has a higher first IP of 13.99 eV. We also found that the microlightning in the microdroplets' atmosphere can also form NO^+ and $NO_2{}^+$ by spraying water microdroplets into the chamber with N_2 and O_2 (note S1 and fig. S7), which is in agreement with the previous work of Banerjee and co-workers (*13*). By using a picoammeter, the current of the water droplet microlightning is also measured (note S2 and fig. S8). Current saturation at high N_2 pressure indicates that the discharge behavior is related to droplet size, which eventually stabilizes at a higher nebulizing gas pressure over than 120 psi (827 kPa).

Microlightning energy evaluation

To further determine the energy of the microlightning from the approaching of oppositely charged water microdroplets, we prepared a mixture of halo-methane and halo-ethane vapor (listed in Fig. 3) with different first IPs. Details are provided in note S1. Figure 3A shows the full mass spectrum, and Figs. 3B and 4H show the zoomed-in mass spectrum of each component in the mixed vapor that is identified. All the molecules can be ionized by microlightning. Because of the different first IPs, each ion has a different intensity. CH_3I has the lowest first IP, which is 9.50 eV. It can be clearly found that CH_3I^+ at *m/z* 141.9263 has the highest intensity as shown in Fig. 3A. As the first IP increases, the signal intensities of the different ions gradually decrease. Figure 3I shows the relationship between the absolute intensity of total ions and first IP of different molecules. The first IP of $CFCl_3$ is 11.77 eV, which makes it more difficult to be ionized by the microlightning between oppositely charged water microdroplets.

In a separate experiment, we did not see ion signals from CH_2F_2 and C_2HF_5 when we introduced halocarbon 410-A gas, which is a mixture of CH_2F_2 and C_2HF_5. This might be because the energy of the microlightning is lower than the first IP of CH_2F_2 (12.7 eV) and C_2HF_5 (12.5 eV) or the lack of sensitivity of the MS used. According to the results we show above, the energy of the microlightning between oppositely charged water microdroplets is between 12.13 (first IP of Xe) and 12.5 eV (first IP of C_2HF_5). It should be mentioned that the above inference is based on the sensitivity of our mass spectrometer.

Generation of reaction products

The transformation of inorganic nitrogen, such as N_2 in the atmosphere, into organic nitrogen compounds on early Earth has long been a subject of scientific inquiry. Since the landmark experiments by Miller and Urey (*21*), many researchers have hypothesized that lightning could play a crucial role in synthesizing life's building blocks from abiotic molecules. High-energy discharges, such as lightning, ionize or dissociate inorganic gases like N_2, CH_4, CO_2, and NH_3 and lead to the formation of radicals and ions that can then react to produce organic compounds (*32*–*38*). In what follows, we show that microlightning from water droplets that are surrounded by gases can act the same way as lightning to cause ionization and chemical transformations.

The homebuilt experimental setup based on an Orbitrap mass spectrometer was used for the in situ generation and detection of organic molecules from the water droplet microlightning (Fig. 4A). An 8:1:1 mixture of N_2, CH_4, and CO_2 is used as the nebulizing gas to generate water microdroplets and microlightning. The stainless steel vessel, which contains an aqueous ammonia solution, is connected to the chamber by a valve. By heating the vessel, NH_3 evaporates into the chamber. Reaction products are directly monitored by the mass spectrometer through the MS inlet.

Figure 4A shows typical pathways for the formation of some organic molecules that we have detected. All reaction products have been observed previously in discharge-bulb experiments. For example, microlightning can lead to bond dissociation of N_2 and CH_4, followed by formation of $\bullet CH_{x\ (x=1\text{-}3)}$ radicals and active nitrogen, which can form hydrogen cyanide (HCN) (note S3 and fig. S9). Furthermore, cyanoacetylene (**I**) forms, which is the second most abundant molecule in the Miller-Urey experiment and one of the most important intermediates in transforming inorganic nitrogen gas to molecules containing C—N bonds. Many studies have proposed possible reaction mechanisms, most of which indicate that the reaction is based on radicals (*38*). Along with hydrolysis and oxidation, cyanoacetylene is transformed into cyanoacetaldehyde (**II**) and cyanoacetic acid (**III**). At the same time, $\bullet CH_3$ can react with •OH to form methanol, which is oxidized to formaldehyde and formic acid. Studies have shown that formic acid reacts with hydrogen cyanide to form glycine (**IV**) (*36*), which is an important amino acid product in the Miller-Urey experiment. In addition, we also detected urea (**V**), which is from the reaction of CO_2 and NH_3 in the chamber. We also observe the formation of uracil (**VI**), which is thought to originate from the reaction of urea with cyanoacetaldehyde followed by subsequent hydrolysis. It is worth mentioning that other products are also possible but not detected because of the detection limits of our mass spectrometer. The distance between the droplet sprayer and the mass spectrometer inlet is set to 10 mm. A previous study has shown that the velocity of sprayed water microdroplets is about 83 m/s under the present nebulizing conditions (*39*). Thus, the reaction products we have observed formed in 120 μs or less.

In a separate experiment, we also collected water vapor under the same gas conditions using a condensate plate. This is a method that produces only single water droplets instead of causing droplet splitting. In this case, we did not observe the formation of HCN. These results confirm that the formation of HCN from N_2 and CH_4 is caused by microlightning between two oppositely charged droplets in close proximity and does not result from the interaction of the surrounding gas with a single microdroplet.

Chemical components of the gas-microdroplet system are directly detected by MS. As shown in Fig. 4B, cyanoacetylene (**I**) is detected in the form of deprotonation (C_3N^-) under negative ion mode at *m/z* 50.0036, which is because the terminal alkynes have relatively high electronegativity. Figure 4C shows the protonated cyanoacetaldehyde (**II**: $C_3H_4NO^+$) at *m/z* 70.0291, which is oxidized

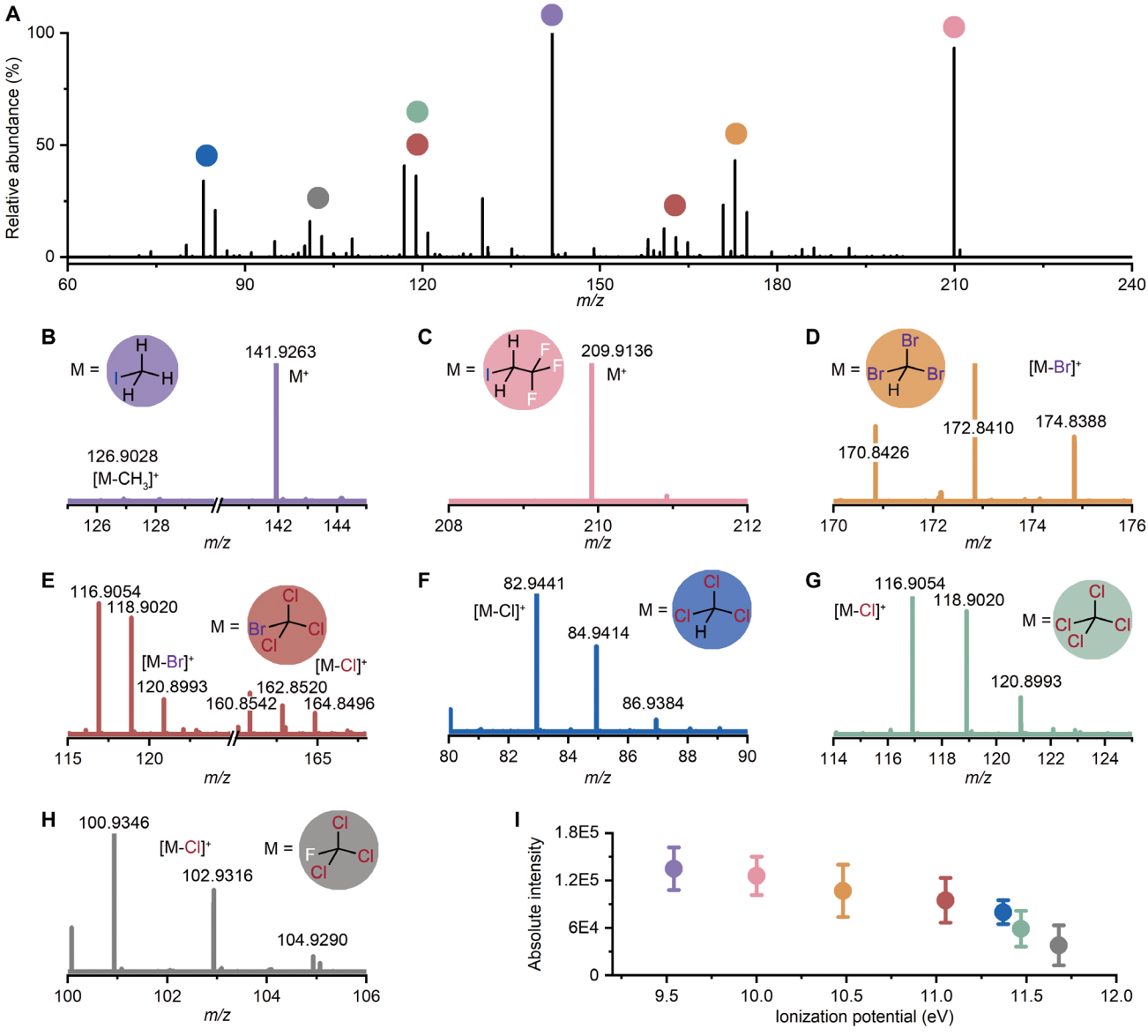

Fig. 3. Evaluation of the energy of microlightning. (**A**) Mass spectrum of chemical components in the chamber when spraying microdroplets to a mixed vapor having equal amounts of CH_3I (purple), CH_2ICF_3 (pink), $CHBr_3$ (orange), $CBrCl_3$ (red), $CHCl_3$ (blue), CCl_4 (light green), and $CFCl_3$ (gray). (**B** to **H**) Zoomed-in mass spectrum of different identified molecules. (**I**) Relationship between the absolute intensity of total ions and first IP of different molecules. Error bars represent the SDs determined from three measurements.

into cyanoacetic acid (**III**: $C_3H_3NO_2$), and the deprotonated ion ($C_3H_3NO_2^-$), which can be detected under negatively ion mode at *m/z* 84.0094 (Fig. 4D). Deprotonated glycine (**IV**) is detected in $C_2H_4NO_2^-$ at *m/z* 74.0249, as demonstrated in Fig. 4E. Urea (**V**) is detected in the form of protonation ($CH_5N_2O^+$) under positive ion mode at *m/z* 61.0399 (Fig. 4F). Uracil (**VI**) is obtained through the reaction of **II** and **V**, followed by subsequent hydrolysis. The protonated uracil is detected in $C_4H_5N_2O_2^+$ at *m/z* 113.0349, which is shown in Fig. 4G. Tandem MS (MS^2) is used to verify the structure of uracil (fig. S10).

DISCUSSION

In conclusion, we have demonstrated that water droplets in a spray generate luminescence, which we call microlightning, when they split into smaller droplets in the absence of any external voltage. This microlightning can excite, dissociate, or ionize the surrounding ground-state molecules, causing chemical reactions to occur in the gas surrounding water microdroplets. When water microdroplets are surrounded by N_2, CH_4, CO_2, and NH_3, we find the same small organic molecules as reported in the classic Miller-Urey experiment and other bulb-discharge experiments studying prebiotic syntheses, which have been postulated to be an important source for making the building blocks of life. In nature, this microlightning caused by droplet splitting is considered to be common, for example, it frequently occurs in ocean waves and around waterfalls. On the basis of what we observed in this study, we suggest that this common energy source may provide a route for creating C—N bonds from abiotic gas molecules expected to be present on early Earth.

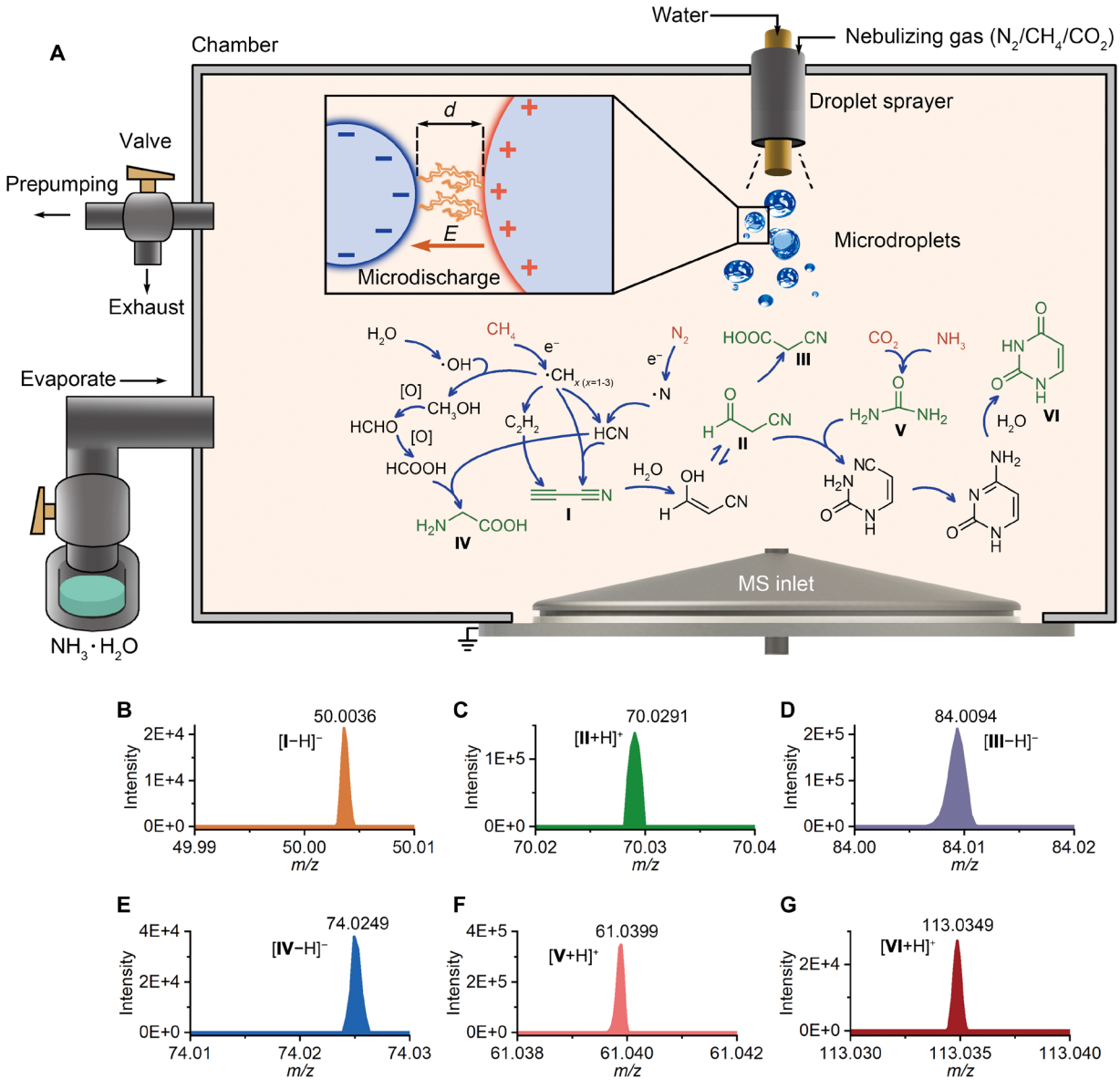

Fig. 4. Prebiotic synthesis by water droplet microlightning. (**A**) Schematic diagram of the prebiotic synthesis experiment. Gases (N_2, CH_4, CO_2, and NH_3) in orange surround a spray containing larger positively and smaller negatively charged water microdroplets, which, when they come into proximity, cause a microlightning, forming the products in green: (**I**) cyanoacetylene, (**II**) cyanoacetaldehyde, (**III**) cyanoacetic acid, (**IV**) glycine, (**V**) urea, and (**VI**) uracil. (**B** to **G**) Mass spectrum of identified molecules marked **I** to **VI** in (A). (B) Deprotonated cyanoacetylene at *m/z* 50.0036. (C) Protonated cyanoacetaldehyde at *m/z* 70.0291. (D) Deprotonated cyanoacetic acid at *m/z* 84.0094. (E) Deprotonated glycine at *m/z* 74.0249. (F) Protonated urea at *m/z* 61.0399. (G) Protonated uracil at *m/z* 113.0349.

MATERIALS AND METHODS

Chemicals and gases

Aqueous ammonia solution, benzene, octane, bromine, iodomethane, 1,1,1-trifluoro-2-iodoethane, bromoform, trichlorobromomethane, chloroform, carbon tetrachloride, and trichloromonofluoromethane were purchased from Sigma-Aldrich (St. Louis, MO, USA). N_2, CH_4, CO_2, and Kr were purchased from Linde Gas & Equipment (Dublin, Ireland). Xe was purchased from Advanced Specialty Gases (Reno, NV, USA).

Materials and equipment

The fused silica capillary was purchased from Polymicro Technologies (Phoenix, AZ, USA). The inner diameter (ID) of the capillary is 75 μm, and the outer diameter (OD) is 375 μm. Cyanide Test Kit was purchased from Sigma-Aldrich (St. Louis, MO, USA).

A green LED (light-emitting diode) light (570 nm) was used as the illumination source. A band-pass filter (450 ± 5 nm) was installed in front of the high-speed camera to prevent the green light from entering the detector. A single droplet was added to the acoustic levitation area. By controlling the distance between the transmitter and the reflector, the original large water droplet split into several smaller droplets. The microlightning from the droplet splitting was recorded by the camera.

A coaxial capillary device is used to generate microdroplets. The spray system consisted of a syringe pump (Masterflex, Cole Parmer, Vernon Hills, IL, USA), a silica capillary, stainless steel tubing (ID:

500 μm, OD: 2 mm, and length: 30 mm) and stainless steel tee (Swagelok, Solon, OH, USA), and gas supply. Deionized water is injected from the central silica capillary with a flow rate of 10 μl/min. The pressure of the nebulizing gas is set to 120 psi (827,371.2 Pa). An Orbitrap high-resolution mass spectrometer (Orbitrap Velos Pro, Thermo Fisher Scientific, Waltham, MA, USA) was used for the online microdroplet reaction monitoring and target product identification. The capillary temperature is set to 275°C. For the detection of nitrogen oxides, a mass spectrometer (LTQ, Thermo Fisher Scientific, Waltham, MA, USA) was used. The *m/z* range was set to "low."

Ionization of benzene

A stainless steel sealed chamber is installed outside the inlet of a mass spectrometer (Orbitrap Velos Pro, Thermo Fisher Scientific, Waltham, MA, USA). The chamber is evacuated by a pump to remove air. A coaxial capillary device is used to generate microdroplets. Deionized water is injected from the central silica capillary with a flow rate of 10 μl/min. Benzene (1 ml) was added into the stainless steel vessel shown in fig. S2. We set the temperature of the vessel at 100°C to ensure the complete volatilization of benzene, whose boiling point is 80.1°C. Water of high purity (99.999%) is injected from the capillary and sprayed into the chamber by N_2 at a pressure of 120 psi (827,371.2 Pa).

Ionization of vapor mixture

Iodomethane (CH_3I), 1,1,1-trifluoro-2-iodoethane (CH_2ICF_3), bromoform ($CHBr_3$), trichlorobromomethane ($CBrCl_3$), chloroform ($CHCl_3$), carbon tetrachloride (CCl_4), and trichloromonofluoromethane ($CFCl_3$) are mixed and added to the vessel at equal concentrations, each with a volume of 100 μl. The container is heated to 200°C, which is higher than the boiling point of the least volatile compound, to ensure that all organic molecules are evaporated and have the same vapor pressure. Water microdroplets are generated from the sprayer at an injection speed of 10 μl/min while the mixed vapor is simultaneously introduced into the chamber. Positive ions produced by the microlightning from the vapor are directly detected by the mass spectrometer.

Supplementary Materials

The PDF file includes:
Supplementary Notes S1 to S3
Figs. S1 to S10
Legends for movies S1 to S8

Other Supplementary Material for this manuscript includes the following:
Movies S1 to S8

REFERENCES AND NOTES

1. W. Thomson, XVI.On a self-acting apparatus for multiplying and maintaining electric charges, with applications to illustrate the voltaic theory. *Proc. R. Soc. Lond.* **16**, 67–72 (1868).
2. E. R. Williams, Large-scale charge separation in thunderclouds. *J. Geophys. Res.* **90**, 6013–6025 (1985).
3. R. Anderson, S. Gathman, J. Hughes, S. Björnsson, S. Jónasson, D. C. Blanchard, C. B. Moore, H. J. Survilas, B. Vonnegut, Electricity in volcanic clouds. *Science* **148**, 1179–1189 (1965).
4. I. Bhattacharyya, J. T. Maze, G. E. Ewing, M. F. Jarrold, Charge separation from the bursting of bubbles on water. *J. Phys. Chem. A* **115**, 5723–5728 (2011).
5. Z. L. Wang, A. C. Wang, On the origin of contact-electrification. *Mater. Today* **30**, 34–51 (2019).
6. S. Lin, X. Chen, Z. L. Wang, Contact electrification at the liquid–solid interface. *Chem. Rev.* **122**, 5209–5232 (2022).
7. J. Lowell, A. C. Rose-Innes, Contact electrification. *Adv. Phys.* **29**, 947–1023 (1980).
8. F. Galembeck, L. P. Santos, T. A. L. Burgo, A. Galembeck, The emerging chemistry of self-electrified water interfaces. *Chem. Soc. Rev.* **53**, 2578–2602 (2024).
9. P. Lenard, Ueber die Electricität der Wasserfälle. *Ann. Phys.* **282**, 584–636 (1892).
10. S. Lin, L. N. Y. Cao, Z. Tang, Z. L. Wang, Size-dependent charge transfer between water microdroplets. *Proc. Natl. Acad. Sci. U.S.A.* **120**, e2307977120 (2023).
11. L. W. Zilch, J. T. Maze, J. W. Smith, G. E. Ewing, M. F. Jarrold, Charge separation in the aerodynamic breakup of micrometer-sized water droplets. *J. Phys. Chem. A* **112**, 13352–13363 (2008).
12. Y. Xia, J. Xu, J. Li, B. Chen, Y. Dai, R. N. Zare, Visualization of the charging of water droplets sprayed into air. *J. Phys. Chem. A* **128**, 5684–5690 (2024).
13. A. Kumar, V. S. Avadhani, A. Nandy, S. Mondal, B. Pathak, V. K. N. Pavuluri, M. M. Avulapati, S. Banerjee, Water microdroplets in air: A hitherto unnoticed natural source of nitrogen oxides. *Anal. Chem.* **96**, 10515–10523 (2024).
14. P. A. Cherenkov, Visible light from clear liquids under the action of gamma radiation. *C.R. (Dokl.) Acad. Sci. URSS* **2**, 451–454 (1934).
15. I. E. Tamm, General characteristics of Vavilov-Cherenkov radiation. *Science* **131**, 206–210 (1960).
16. B. K. Spoorthi, K. Debnath, P. Basuri, A. Nagar, U. V. Waghmare, T. Pradeep, Spontaneous weathering of natural minerals in charged water microdroplets forms nanomaterials. *Science* **384**, 1012–1017 (2024).
17. D. T. Holden, N. M. Morato, R. G. Cooks, Aqueous microdroplets enable abiotic synthesis and chain extension of unique peptide isomers from free amino acids. *Proc. Natl. Acad. Sci. U.S.A.* **119**, e2212642119 (2022).
18. S. Jin, H. Chen, X. Yuan, D. Xing, R. Wang, L. Zhao, D. Zhang, C. Gong, C. Zhu, X. Gao, Y. Chen, X. Zhang, The spontaneous electron-mediated redox processes on sprayed water microdroplets. *JACS Au* **3**, 1563–1571 (2023).
19. A. M. Deal, R. J. Rapf, V. Vaida, Water–air interfaces as environments to address the water paradox in prebiotic chemistry: A physical chemistry perspective. *J. Phys. Chem. A* **125**, 4929–4942 (2021).
20. S. L. Miller, A production of amino acids under possible primitive earth conditions. *Science* **117**, 528–529 (1953).
21. S. L. Miller, H. C. Urey, Organic compound synthesis on the primitive earth. *Science* **130**, 245–251 (1959).
22. K. J. Baeyens, H. L. De Bondt, S. R. Holbrook, Structure of an RNA double helix including uracil-uracil base pairs in an internal loop. *Nat. Struct. Biol.* **2**, 56–62 (1995).
23. P. Sunka, V. Babický, M. Clupek, P. Lukes, M. Simek, J. Schmidt, M. Cernák, Generation of chemically active species by electrical discharges in water. *Plasma Sources Sci. Technol.* **8**, 258–265 (1999).
24. Y. Jin, C. Wu, P. Sun, M. Wang, M. Cui, C. Zhang, Z. Wang, Electrification of water: From basics to applications. *Droplet* **1**, 92–109 (2022).
25. J. Nauruzbayeva, Z. Sun, A. Gallo, M. Ibrahim, J. C. Santamarina, H. Mishra, Electrification at water–hydrophobe interfaces. *Nat. Commun.* **11**, 5285 (2020).
26. V. Artemov, L. Frank, R. Doronin, P. Stärk, A. Schlaich, A. Andreev, T. Leisner, A. Radenovic, A. Kiselev, The three-phase contact potential difference modulates the water surface charge. *J. Phys. Chem. Lett.* **14**, 4796–4802 (2023).
27. H. Conrads, M. Schmidt, Plasma generation and plasma sources. *Plasma Sources Sci. Technol.* **9**, 441–454 (2000).
28. A. Albert, C. Engelhard, Characteristics of low-temperature plasma ionization for ambient mass spectrometry compared to electrospray ionization and atmospheric pressure chemical ionization. *Anal. Chem.* **84**, 10657–10664 (2012).
29. X. Chen, Y. Xia, Z. Zhang, L. Hua, X. Jia, F. Wang, R. N. Zare, Hydrocarbon degradation by contact with anoxic water microdroplets. *J. Am. Chem. Soc.* **145**, 21538–21545 (2023).
30. P. Potzinger, G. Von Bünau, Empirische Berücksichtigung von Überschußenergien bei der Auftrittspotentialbestimmung. *Ber. Bunsenges. Phys. Chem.* **73**, 466–473 (1969).
31. National Institute of Standards and Technology, Octane, https://webbook.nist.gov/cgi/cbook.cgi?ID=C111659&Mask=20.
32. R. Shapiro, Prebiotic cytosine synthesis: A critical analysis and implications for the origin of life. *Proc. Natl. Acad. Sci. U.S.A.* **96**, 4396–4401 (1999).
33. M. P. Robertson, S. L. Miller, An efficient prebiotic synthesis of cytosine and uracil. *Nature* **375**, 772–774 (1995).
34. J. L. Bada, Volcanic Island lightning prebiotic chemistry and the origin of life in the early Hadean eon. *Nat. Commun.* **14**, 2011 (2023).
35. H. J. Jiang, T. C. Underwood, J. G. Bell, J. Lei, J. C. Gonzales, L. Emge, L. G. Tadese, M. K. Abd El-Rahman, D. M. Wilmouth, L. C. Brazaca, G. Ni, L. Belding, S. Dey, A. A. Ashkarran, A. Nagarkar, M. P. Nemitz, B. J. Cafferty, D. S. Sayres, S. Ranjan, D. R. Crocker, J. G. Anderson, D. D. Sasselov, G. M. Whitesides, Mimicking lightning-induced electrochemistry on the early Earth. *Proc. Natl. Acad. Sci. U.S.A.* **121**, e2400819121 (2024).
36. A. Sato, Y. Kitazawa, T. Ochi, M. Shoji, Y. Komatsu, M. Kayanuma, Y. Aikawa, M. Umemura, Y. Shigeta, First-principles study of the formation of glycine-producing radicals from common interstellar species. *Mol. Astrophys.* **10**, 11–19 (2018).

37. N. Kitadai, S. Maruyama, Origins of building blocks of life: A review. *Geosci. Front.* **9**, 1117–1153 (2018).
38. R. A. Sanchez, J. P. Ferris, L. E. Orgel, Cyanoacetylene in prebiotic synthesis. *Science* **154**, 784–785 (1966).
39. J. K. Lee, S. Kim, H. G. Nam, R. N. Zare, Microdroplet fusion mass spectrometry for fast reaction kinetics. *Proc. Natl. Acad. Sci. U.S.A.* **112**, 3898–3903 (2015).

Acknowledgments: We thank X. Zhang, College of Chemistry, Nankai University for assistance in building the droplet levitation setup. **Funding:** This study was supported by the Air Force Office of Scientific Research through the Multidisciplinary University Research Initiative (MURI) program (AFOSR FA9550-21-1-0170) and National Natural Science Foundation of China (22306073). **Author contributions:** R.N.Z. conceived on this study. Y.M. and R.N.Z. designed the experiments and wrote the initial draft. Y.M. and Y.X. performed data collection and analysis. Y.X. and J.X. contributed to the simulation. **Competing interests:** The authors declare that they have no competing interests. **Data and materials availability:** All data needed to evaluate the conclusions in this paper are present in the paper and/or the Supplementary Materials.

Submitted 15 October 2024
Accepted 6 February 2025
Published 14 March 2025
10.1126/sciadv.adt8979